

Mahya Safarzadeh¹, Shahed Taheri²
and Gity Mir Mohamad Sadeghi^{1*}

¹Department of Polymer Engineering & Color
Technology, Amirkabir University of Technology,
Tehran, Iran

²Department of Biomedical Engineering, Amirkabir
University of Technology, Tehran, Iran

Dates: Received: 13 December, 2016; Accepted: 09
January, 2017; Published: 11 January, 2017

*Corresponding author: Gity Mir Mohamad Sadeghi,
Amirkabir University of Technology, Department of
Polymer Engineering, 424 Hafez Ave, Tehran, Iran,
Tel: +98 21 64542442; Fax: +98 21 66468243; E-mail:
gsadeghi@aut.ac.ir

Keywords: Chitosan nanoparticle; Human umbilical
valve endothelial cells; Ultrasonication; Drug carriers;
In vitro studies

<https://www.peertechz.com>

Research Article

Highly Monodisperse Chitosan Nanoparticles Prepared by a Combined Triple-Method for Potential Use as Drug Carriers

Abstract

Chitosan (CS) as a biodegradable polymer with unique bio-attachment properties that makes it favorable to be used in biomedical applications. Insolubility in water is the problem with use of CS. The purpose of this study was to prepare low molecular weight, water-soluble CS nanoparticles that exhibit excellent water solubility and biological, chemical, and physical functions. Oxidative degradation technique using hydrogen peroxide (H₂O₂) was used to decrease chitosan molecular weight. Then ultrasonication and ionic gelation method using sodium tripolyphosphate (TPP) were used to prepare CS nanoparticles. Molecular weight of chitosan determined by Ubbelohde viscometry and it decreased by approximately 100%. From the spectral information (FTIR) it was observed that the cross-linking between CS and TPP was taking place while the main structure of chitosan was the same. The dynamic light scattering results showed that water-soluble nanoparticles had a multimodal size distribution pattern, while low molecular particles yielded monodisperse particle distribution with an average size of ~45 nm, which was directly ascribed to the role of ultrasonication process. The morphology of nanoparticles was observed by SEM and TEM techniques. The mean diameter of nanoparticles was obtained in a range of 30 nm to 45 nm with a narrow size distribution and polydispersity index smaller than 0.2. Cytotoxicity of CS nanoparticles on human umbilical valve endothelial cells (HUVEC) was assessed by CCK-8 assay, as well as "Live/Dead" assay and subsequent fluorescent imaging. The results showed no to minimal cytotoxicity for CS solutions up to 50 µg/ml, while sporadic dead cells observed for 100 µg/ml solutions. This suggested that our monodisperse nanoparticle systems are great candidates to be used for drug delivery systems.

Introduction

Chitosan (CS) is a high molecular weight polysaccharide composed of β-(1,4)-2-acetamido-2-deoxy-D-glucose and β-(1,4)-2-amino-2-deoxy-D-glucose units. It is a natural polymer, non-toxic, biodegradable, which has been found a fascinating candidate in a broad spectrum of applications such as targeted drug delivery, wound dressing, tissue and cell engineering, radiopharmaceuticals and cosmetic industries, along with unique biological properties including biocompatibility, physiological inertness, remarkable affinity to proteins, antibacterial, haemostatic, fungistatic, anti-tumoral and anticholesteremic properties [1-3]. In the form of microparticles and nanoparticles, CS has a variety of important applications. Loaded with DNA plasmids, CS nanoparticles could give rise to protective immune responses in rodents [4]. Likewise, the use of CS nanoparticles as nanomedicine and drug carriers has been extensively reported before [5-7]. For example, insulin-loaded chitosan nanoparticles could enhance

intestinal absorption of insulin and increase its relative pharmacological bioavailability [8]. In enhancing gene-transfer efficiency in cells, CS nanoparticles have been proved to be valuable assets [9].

However, due to its high molecular weight and viscosity, chitosan has a low solubility (above pH 6.5) in a variety of solvents, which limit its applications, especially when functionalities such as "lipid binding" is required (nanomedicine and targeted drug delivery) [10]. To overcome this issue, a popular approach is to reduce the molecular weight of chitosan. It has been reported that low molecular weight chitosan (LWCS) shows an outstanding water solubility and biological, chemical, and physical functionality, providing that its chemical structure is not changed [11]. A common synthetic rout to obtain LWCS is enzymatic degradation of CS with hydrolytic enzymes or acidic degradation by hydrochloric acid and sulfuric acid [12,13]. Recently, LWCS was also formed by oxidative degradation with some oxidative systems [14-16]. The degradation patterns of chitosan using O₃ and NaNO₂

have been reported [14,15]. Tanioka et al. [16], and Chang et al. [17], respectively reported that Cu (II)-UV-H₂O₂ and H₂O₂-Fe²⁺ systems could decrease the molecular weights of chitosan. They postulated that metal ions induced the decomposition of H₂O₂, which caused the degradation. Nonetheless, the capacity of chitosan to form complexes with metallic ions has made ionic-metal-driven oxidative systems less desirable; especially when it comes to biomedical application [18]. On the other hand, when H₂O₂ is used alone, oxidative degradation is an inefficient method to obtain a monodisperse nanoparticle system. To improve the efficiency, we propose a triple-method treatment of oxidative degradation, ultrasonication and ionic gelation.

The use of ultrasonication in nanotechnology has been ubiquitous in recent years. Nevertheless, its effects on CS nanoparticles are not well understood, in spite of a plethora of research works that are devoted to ultrasound-assisted techniques in CS nanoparticle preparation. Also, the ionic gelation method has been separately used to prepare CS nanoparticles. Bodmeier et al. [19], was the first to report the ionic gelation of chitosan using sodium tripolyphosphate (TPP), while Alonso et al. [20] developed chitosan nanoparticles by adding a solution containing TPP into an acidic phase (pH 4-6) containing CS. The study of Wu et al. [21], showed that the formation of nanoparticles is possible only within specific, moderate concentrations of chitosan and TPP. Furthermore, the chitosan/TPP weight ratio should be within the range of 4:1-6:1 in order to obtain a high yield of nanoparticles [22]. The study of Tsai et al. [23], showed that the particle size of chitosan nanoparticles prepared by the ionic gelation method can be influenced by using different mechanical energies such as ultrasonic radiation or mechanical shearing, different treatment times, different chitosan concentrations, and different solution temperatures.

Despite a relatively large work that has been conducted in this area, a series of deficiencies still prevail. For example, the feasibility of producing LWCS by using hydrogen peroxide has been overlooked due to the additional procedures that it requires. Moreover, the use of parallel techniques to reach the optimum system in terms of parameters such as mean average size, Zeta potential, and uniformity has been minimal. Taking the antecedents into account, the aim of the present study is to prepare low molecular weight, water-soluble chitosan nanoparticles by means of a unique combined treatment of oxidative degradation, ultrasonication and ionic gelation. Specifically, achieving an extremely narrow size distribution is one of the priorities of the current research, since a narrow distribution is vital in drug delivery to ensure identical biological response by each particle.

Experimental

Materials

Middle-viscous crab shell chitosan (CS) was purchased from Sigma-Aldrich (United States, cat. no. 28191). Hydrochloric acid fuming 37% (HCl), acetic acid (glacial) 100%, (AA), sodium chloride (NaCl), and hydrogen peroxide

30% (H₂O₂) were purchased from Merck, Germany. Sodium tripolyphosphate (TPP) was purchased from Sigma-Aldrich, Germany, and sodium hydroxide (NaOH) was purchased from Chem-Lab, Belgium. Human umbilical vein endothelial cells (HUVECs) were kindly provided by the National Cell Bank of Iran. Cells were cultured by standard protocols. A combination of Dulbecco's modified Eagle's medium (DMEM, Gibco, USA), Ham's F12 (Gibco, USA) with 10% fetal bovine serum (FBS, Gibco, USA) were used as culture medium and cells were incubated in 37 °C, 90% humidity in air plus 5% CO₂.

Chitosan degradation and ultrasonication

Chitosan solution (2%) was prepared in 0.1 M HCl by stirring for 24 h in room temperature. A solution of H₂O₂ 30% (4.4%) was then used to achieve chemical degradation of chitosan in 30 for 1.5 h. Adjusting the pH of the solution to approximately 7 was carried out by using 1 M NaOH solution. As the pH increased, part of chitosan was precipitated. Hence, the solution was centrifuged at 6000 rpm for 30 minutes to separate sediments. The upper phase of the centrifuged solution included water-soluble chitosan (WSCS), which was soluble in neutral pH, and the lower phase consisted of low molecular weight chitosan (LWCS).

Then, WSCS was vacuum filtered with the aid of appropriate filter paper, while the LWCS was submitted to ultrasonic irradiation with an amplitude of 100 Hz for 20 minutes in order to break the chains further.

Ionic gelation

Ionic gelation was carried out for both LWCS and WSCS. The pH of the solution was adjusted to approximately 5 by the addition of acetic acid. Then, the TPP solution was added to the chitosan solution drop wise until the resulting mixture became opaque. For separating nanoparticles from microparticles, the solution was centrifuged at 6000 rpm for 30 minutes again. The upper phase was filtered by means of syringe filters with two different mesh sizes (450 nm and 220 nm). The filtered solution was freeze-dried for 72 hours to be used for further uses. The prepared samples were named indicating the type of nanoparticles and the used mesh size, as WSCS-450 or LWCS-220 stand for water-soluble nanoparticles that were filtered by a 450 nm mesh size, and low molecular weight CS nanoparticles that were filtered by a 220 nm mesh size and were submitted to ultrasonic irradiation, respectively.

Characterization

Chitosan nanoparticles were characterized by a Bruker EQUINOX 55 infrared spectrophotometer (FTIR). The spectra were acquired with a signal resolution of 2 cm⁻¹ within the 4000-400 cm⁻¹ range. The number of scans was set at 20 for each sample. The Intrinsic viscosity and molecular weight of chitosan were measured with a Cannon-Ubbelohde Viscometer Size 2C, based on the viscometric constants in the Mark-Houwink equation [24].

$$[\eta]=k M_v^\alpha \quad (1)$$

Where $[\eta]$ is the intrinsic viscosity and M_v is viscosity molecular weight of polymer. In order to calculate the M_v , k and α are assumed to be constant (1.81×10^{-3} mL/g and 0.93, respectively) in a solvent system of 0.1 M $\text{CH}_3\text{COOH}/0.2$ M NaCl at 25°C [25]. An AIS2100C scanning electron microscope (SEM) was used to evaluate the surface morphology of nanoparticles. One drop of each chitosan solutions was put to the glass lam, dried at room temperature, gold-coated and prepared for SEM. Transmission electron microscopy (TEM) was performed to monitor the shape and structure of water-soluble nanoparticles more accurately. The samples were immobilized on copper grids and dried at room temperature before testing by a Philips EM400 electron microscope. The mean size, size distribution and zeta potential of each nanoparticle suspensions were analyzed using dynamic light scattering (DLS) and zeta potential analyzing, with a Brookhaven ZetaPlus device. The cytotoxicity of the synthesized CS nanoparticles was examined by a Cell Counting Kit-8 (CCK-8) assay. Human umbilical valve endothelial cells (HUVEC) at a density of 3×10^4 cells per well were seeded into 96-well culture plates, in a 100 μl FBS culture medium for 48 h. The medium was removed and replenished with fresh media containing HUVECs, which were incubated with various concentrations of autoclaved CS nanoparticles (5–100 $\mu\text{g}/\text{ml}$). After 24 h, the CS nanoparticles were removed, the cells were washed and were further assessed for viability using a CCK-8 assay. CCK-solution (10 μl) was added to each well, followed by incubation for 3h at 37 °C. The absorbance at a wavelength of 450 nm was measured by a microplate reader (SpectraMax® M5, USA). Three independent experiments of each sample were carried out and the mean \pm SD values were reported. The cell viability was expressed by comparison with the control well, which contained only the cells. The cytotoxicity was further evaluated by a “Live/Dead” cell viability assay containing typical amounts of Calcein-AM (5 μL) and ethidium homodimer-1 (20 μL). A fluorescence microscope (Olympus, Melville, NY) was then used to detect live (green) and dead (red) cells. In terms of other instrumentations, a Hettich® EBA 20 centrifuge was used for separation purposes, a Hielscher UP100H ultrasonic processor was used to break CS chains, a Metrohm device was employed to measure pH, and an OPERON device was used as freeze dryer.

Results and Discussion

Table 1 shows the intrinsic viscosity and molecular weight of CS and its different nanoparticle samples. As shown by the results, the molecular weight of WSCS system was decreased by 97.8% compared to the pure CS, while LWCS experienced an analogous degree of M_v reduction in the order of 98.1%. This indicates that the decrease of chitosan polysaccharide chain length occurred successfully. Interestingly, the ultrasonication process did not reduce the molecular weight further, as indicated by the higher M_v of LWCS compared to WSCS.

The FTIR spectra of CS and chitosan nanoparticles (LWCS-450 and WSCS-450) are illustrated in Figure 1. The characteristic band associated with the combined peaks of the NH_2 and OH group stretching vibration in original chitosan is seen at 3435 cm^{-1} . The peaks of the CS that appear at, 1647,

1379, and 1080 cm^{-1} are attributed to the carbonyl, methyl, and C–O stretching vibrations, respectively [11]. It was particularly important to detect the 1647 cm^{-1} band, which showed that the carbonyl group is formed during the degradation of chitosan. Vibrations in the range of 1154–896 cm^{-1} are assigned to the characteristics of chitosan’s polysaccharide structure [11]. In comparison with the spectrum of CS, those of LWCS and WSCS revealed almost all of the characteristic vibrations of the original chitosan, indicating that the chemical structure of chitosan was not changed. A few changes about the intensity and wavenumber of a given peak might be due to the destruction of the intramolecular and intermolecular hydrogen bonds and the decrease in the degree of crystallinity in the polymer [11]. Specifically, an additional weak peak in the spectrum at 1250 cm^{-1} is observed for LWCS-450, which can be assigned to the –P=O stretching vibration indicating the presence of phosphate group in the prepared particles. This can verify that the cross-linking took place through the ionic interaction between the negatively charged –P–O– moieties of the phosphate group and protonated NH_3^+ moieties of the chitosan molecule [26]. Furthermore, the 1567 cm^{-1} peak of the stretching vibration of amino groups of chitosan is sharper (in LWCS) than the peak at 1647 cm^{-1} (in CS), showing the high degree of deacetylation of the low molecular weight chitosan nanoparticles. Likewise, a shift from 3445 to 3435 cm^{-1} is shown, and the peak is sharper in the LWCS nanoparticles, which shows that the hydrogen bonding is enhanced. These minimal changes substantiate that the main chemical structure of nanoparticles is sustained.

To analyze the effect of combined treatments of CS on the formation of chitosan nanoparticles, the variations in size, size distribution, and Zeta potential were examined using DLS. The size distribution of different nanoparticle systems, as well as the corresponding PDI values are shown in Figure 2a–d. The WSCS-220 sample showed a bimodal nanoparticle size distribution with average sizes of 29.4 and 62.0 nm. Nevertheless, the small volume fraction of the bigger particles (24%) and the narrow size distribution (PDI = 0.158) can lead to the conclusion that a relatively uniform system was achieved for the aforementioned sample. By increasing the mesh size, the average size distribution and PDI both increased expectedly.

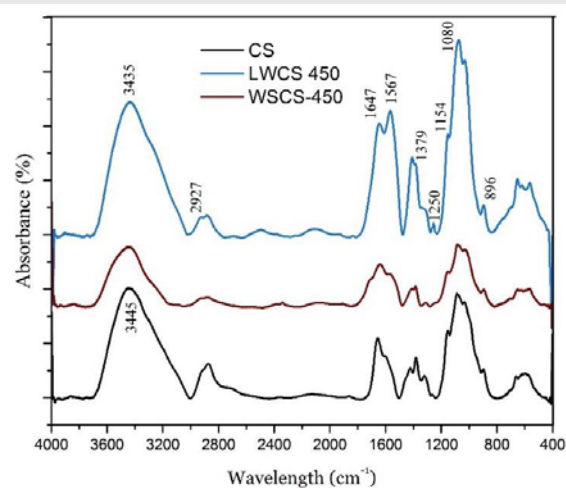


Figure 1: FTIR spectra of CS, LWCS-450 and WSCS-450.

As shown in Figure 2b, the majority of particles had a mean size of 35.4 nm, while three other modes of distribution, with sizes between 29.8–46.1 nm, were observed in the close vicinity of the predominant region. The increase of dispersity value to 0.198 for the WSCS-450 system showed that the particles were fairly heterogenous but in a very limited size range (max size difference of = 16.3 nm).

For the LWCS samples, the only change in preparation procedure compared to WSCS was the addition of an ultrasonication step right before ionic gelation. Hence, Figure 2c,d, reveal the effect of ultrasonic irradiation on the size distribution of CS nanoparticles. As can be seen, for both LWCS-220 and LWCS-450 samples, carefully-controlled monodisperse nanoparticle systems were obtained. LWCS-220 had a single peak for 44.0-nm-sized particles with an extremely narrow size distribution of 0.126. Likewise, LWCS-450 exhibited a unimodal particle size distribution with an average size of 45.7 nm, and a PDI value of 0.149. Comparison of WSCS samples with their LWCS counterparts suggests that ultrasonication had a minimal (if any) effect on reducing the mean average sizes of major modes. Instead, it remarkably contributed to the uniformity of nanoparticles by breaking down the particles in minor modes. This phenomenon can be ascribed to a widely-popular idea that ultrasonication causes main chain scissions at the 1,4-glycosidic bond without affecting the degree of deacetylation of chitosan samples [27].

From Table 1, it can be seen that the Zeta potential for both systems were between 30–36 mV. This suggests that the electrostatic repulsion between neighboring particles were intense enough to yield a stable solution. Achieving stable, positively-charged CS nanoparticles is particularly important in drug delivery applications and cell-polymer interactions, where the cell membrane is often negatively charged [28].

The SEM micrographs of CS nanoparticles derived from corresponding thick solutions (LWCS, and WSCS) are shown in Figure 3a,b. Due to the high concentration and high viscosity of solutions, particles agglomerated and a unique “flowerlike” cluster of particles (marked in the Figure by arrows) became

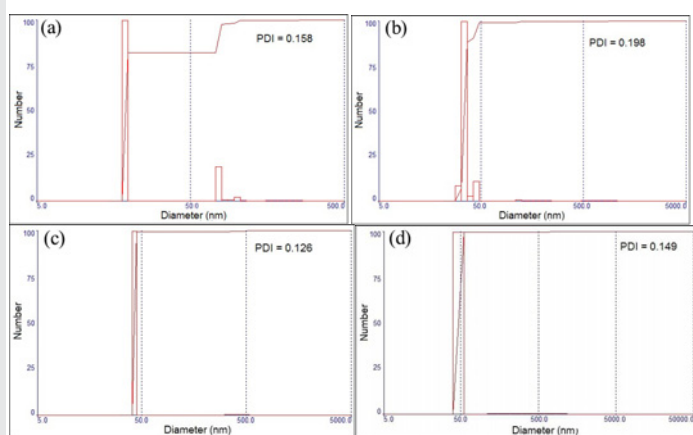


Figure 2: Dynamic light scattering results of (a) WSCS-220, (b) WSCS-450, (c) LWCS-220, and (d) LWCS-450 nanoparticles showing mean size distributions and PDI values.

Table 1: Intrinsic viscosity and molecular weight of CS, WSCS-450, LWCS-450.

Sample	Intrinsic viscosity, $[\eta]$	Molecular weight, M_v (kDa)	Zeta potential (mV)
CS	553.98	792	–
WSCS-450	13.85	15	35.77
LWCS-450	15.56	17	31.14

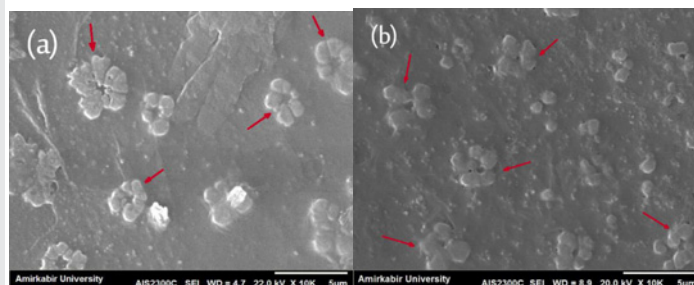


Figure 3: SEM images (a) WSCS (b) LWCS derived from their corresponding “thick” solutions

the predominant feature of the graphs. However, when the solutions were diluted by distilled water, the nanostructure of particles became evident. Partial polydispersity of CS nanoparticles is visible in Figure 4a,b for the WSCS system, with bigger particles appearing in the form of white bright objects, while smaller, uniform nanoparticles created a coarse structure, which is characteristic of surfaces containing nanoparticles [29]. Figure 5 shows a typical TEM image of the WSCS-450 sample. The nanoparticles had a spherical shape, smooth surface, and nanoparticle sizes of 30–50 nm, which was in a good accordance with the results obtained by light scattering technique. Figure 4c,d displayed the monodisperse quality of CS particles that were treated with ultrasonication (LWCS). This implied that ultrasonication had a clear influence on the homogeneity of particle distribution.

Cytotoxicity of the CS nanoparticles was evaluated using CCK-8. The fundament of CCK-8 assay is the conversion of a water-soluble tetrazolium salt, 2-(2-methoxy-4-nitrophenyl)-3-(4-nitrophenyl)-5-(2,4-disulphophenyl)-2H-tetrazolium, monosodium salt (WST-8), to a water-soluble formazan dye upon reduction by dehydrogenases in the presence of an electron carrier [30]. Figure 6a shows the percentage of viable human umbilical valve endothelial cells as a function of the CS concentration (WSCS-220). Overall, the toxic effect of CS nanoparticles was moderate ($CV > 90\%$) at concentrations of up to 50 $\mu\text{g}/\text{ml}$. However, the percentage of viable cells reduced to 84% when the concentration of CS nanoparticles was 100 $\mu\text{g}/\text{ml}$. This is in accordance with the general trend observed for chitosan solutions, which indicates that toxicity is mostly dose-dependent [31,32]. The manifestation of dose-dependent behavior emphasizes a basic principle of toxicology first expressed by Paracelsus, saying that “The dose makes the poison”. The cytotoxic effect of CS on cells followed an analogous pattern for LWCS-220 solution (Figure 6b). However, it can be observed that cell viability was slightly higher in comparison to WSCS-200 sample for all CS concentrations. Interestingly, ultrasonic-assisted CS nanoparticles (LWCS-220) further facilitated cell

proliferation at concentration of 5 $\mu\text{g/ml}$, indicating the good biocompatibility of CS nanoparticles in low dosages for use as drug carriers. Figure 6c shows the fluorescent imaging of the Live/Dead cell assay. The dose-dependent reduction of live cells, which was previously observed by the CCK-8 assay is clearly seen in the micrographs. At 5 $\mu\text{g/ml}$, no to minimal cytotoxicity was observed on endothelial cells, as indicated by the uniformity of alive (green) cells. Nevertheless, sporadic dead (red) cells appeared as the concentration of CS increased. The most intense region of dead cells was observed for the WSCS-220 sample at 100 $\mu\text{g/ml}$, which is in agreement with the results obtained earlier. Overall, the new route to synthesize monodisperse CS nanoparticles can be considered a promising means for the future of drug delivery realm.

Conclusion

In order to address the insolubility of chitosan (CS) in water, chitosan nanoparticles are prepared using a unique combination of H_2O_2 -assisted degradation, ultrasonication (LWCS samples only), and ionic gelation. Molecular weight of chitosan is decreased approximately 100% during the process. From the spectral information (FTIR) it is concluded that the cross-linking between CS and TPP takes place, while the main

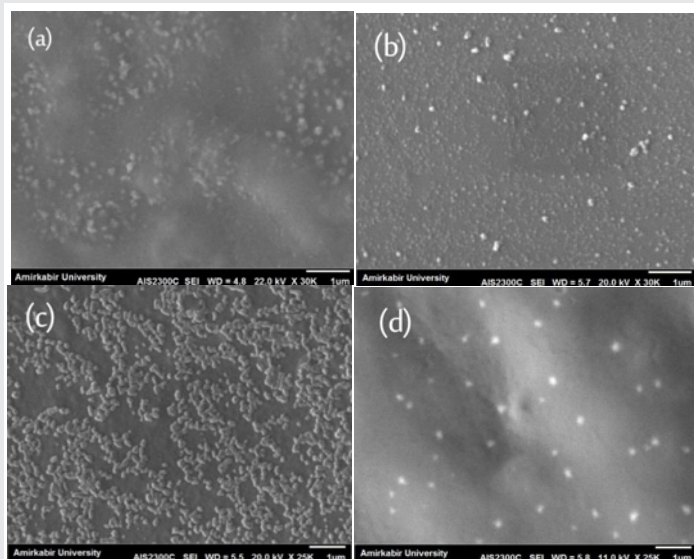


Figure 4: SEM images of diluted solutions containing CS nanoparticles: (a) WSCS-450 (b) WSCS-220 (c) LWCS-450 (d) LWCS-220

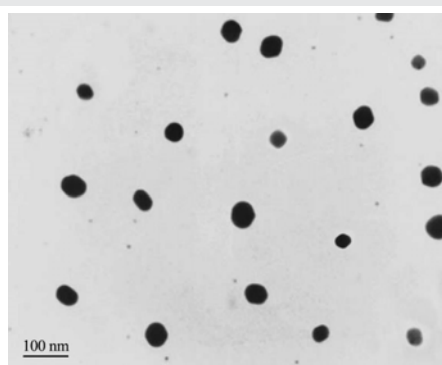


Figure 5: TEM image of the WSCS-450 sample.

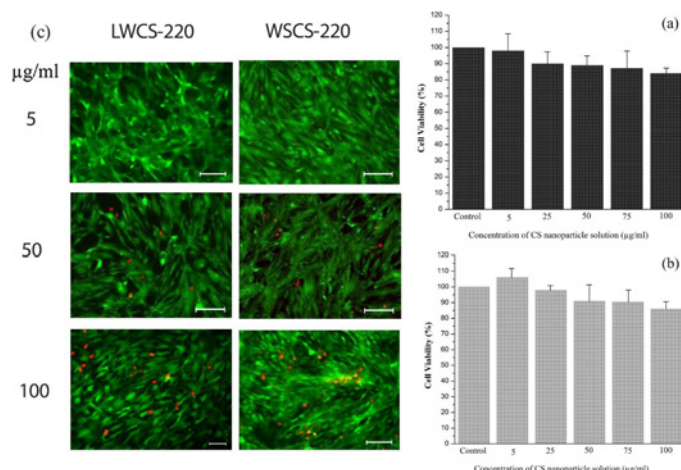


Figure 6: In vitro cytotoxicity assessments of viability of HUVEC cell line (a) CCK-8 assay evaluation of cells incubated with WSCS-220 solution (b) CCK-8 assay evaluation of cells incubated with LWCS-220 solution, and (c) results of the Live/Dead cell assay and the subsequent fluorescent imaging at various CS concentrations

structure of chitosan is unaltered. The DLS results show that WSCS nanoparticles have a multimodal size distribution pattern, although the range of different size modes is very small (16–32 nm). On the other hand, LWCS yields monodisperse particle distribution with an average size of ~ 45 nm, which is directly attributed to the role of ultrasonication process. According to SEM images, the particles agglomerate when thick solutions are used. Upon dilution by distilled water, however, nanoparticles can be seen. *In vitro* cytotoxicity assessments verified the biocompatibility of CS solutions for human umbilical valve endothelial cells up to 50 $\mu\text{g/ml}$ concentration. Overall, nanoparticles with identical, spherical geometries, aqueous solubility, the size distribution as small as 0.126, and the mean positive surface charge of 33 mV can be considered a perfect candidate for drug release and pharmacokinetics applications.

Acknowledgments

This work was partially supported by the Iran Nanotechnology Initiative Council (INIC). We would also like to thank Professor. Hamid Mirzadeh for his consultants.

References

- Katas H, Alpar HO (2006) Development and characterisation of chitosan nanoparticles for siRNA delivery. *J Controlled Release* 115: 216–225. [Link: https://goo.gl/QwyuFQ](https://goo.gl/QwyuFQ)
- Gazori T, Khoshayand MR, Azizi E, Yazdizade P, Nomani A, Haririan I (2009) Evaluation of Alginate/Chitosan nanoparticles as antisense delivery vector: formulation, optimization and in vitro characterization. *Carbohydr. Polym.* 77: 599–606. [Link: https://goo.gl/kDBJwT](https://goo.gl/kDBJwT)
- Mitra S, Gaur U, Ghosh PC, Maitra AN (2001) Tumour targeted delivery of encapsulated dextran–doxorubicin conjugate using chitosan nanoparticles as carrier. *J Controlled Release* 74: 317–323. [Link: https://goo.gl/zyAA4D](https://goo.gl/zyAA4D)
- Roy K, Mao HQ, Huang SK, Leong KW (1999) Oral gene delivery with chitosan–DNA nanoparticles generates immunologic protection in a murine model of peanut allergy. *Nat. Med.* 5: 387–391. [Link: https://goo.gl/W1JzVE](https://goo.gl/W1JzVE)
- Janes KA, Fresneau MP, Marazuela A, Fabra A, Alonso MJ (2001) Chitosan

- nanoparticles as delivery systems for doxorubicin. *J Controlled Release*. 73: 255-267. [Link: https://goo.gl/SfG4wj](https://goo.gl/SfG4wj)
6. De Campos AM, Sánchez A, Alonso MJ (2001) Chitosan nanoparticles: a new vehicle for the improvement of the delivery of drugs to the ocular surface. Application to cyclosporin A. *Int J Pharm* 224: 159-168. [Link: https://goo.gl/asqUCa](https://goo.gl/asqUCa)
 7. Xu Y, Du Y (2003) Effect of molecular structure of chitosan on protein delivery properties of chitosan nanoparticles. *Int J Pharm*. 250: 215-226. [Link: https://goo.gl/cX4CGR](https://goo.gl/cX4CGR)
 8. Pan Y, Li Y, Zhao H, Zheng J, Xu H, et al. (2002) Bioadhesive polysaccharide in protein delivery system: chitosan nanoparticles improve the intestinal absorption of insulin in vivo. *Int J Pharm* 249: 139-147. [Link: https://goo.gl/Xsslep](https://goo.gl/Xsslep)
 9. Kim TH1, Park IK, Nah JW, Choi YJ, Cho CS (2004) Galactosylated chitosan/DNA nanoparticles prepared using water-soluble chitosan as a gene carrier. *Biomaterials* 25: 3783-3792. [Link: https://goo.gl/8WHfyM](https://goo.gl/8WHfyM)
 10. Qi L, Xu Z, Jiang X, Hu C, Zou X (2004) Preparation and antibacterial activity of chitosan nanoparticles. *Carbohydr Res* 339: 2693-2700. [Link: https://goo.gl/88myUd](https://goo.gl/88myUd)
 11. Huang QZ, Meng ZH, Feng YQ, Shi HZ (2010) Study on the heterogeneous degradation of chitosan with H₂O₂ catalyzed by a new supermolecular assembly crystal: [C₆H₈N₂]₆H₃[PW₁₂O₄₀]·2H₂O. *Carbohydr. Res.* 345: 115-119. [Link: https://goo.gl/c6tV1n](https://goo.gl/c6tV1n)
 12. Vårum KM, Antohonsen MW, Grasdalen H, Smidsrød O (1991) Determination of the degree of N-acetylation and the distribution of N-acetyl groups in partially N-deacetylated chitins (chitosans) by high-field nmr spectroscopy. *Carbohydr. Res.* 211: 17-23. [Link: https://goo.gl/esD6LQ](https://goo.gl/esD6LQ)
 13. Rupley JA (1964) The hydrolysis of chitin by concentrated hydrochloric acid, and the preparation of low-molecular-weight substrate for lysozyme. *Biochim Biophys Acta* 83: 245-255. [Link: https://goo.gl/AFS3uN](https://goo.gl/AFS3uN)
 14. Kabal'Nova NN, Murinov KY, Mullagaliev I, Krasnogorskaya N, Shereshovets V, et al. (2001) Oxidative destruction of chitosan under the effect of ozone and hydrogen peroxide. *J Appl Polym Sci* 81: 875-881. [Link: https://goo.gl/jlghQ5](https://goo.gl/jlghQ5)
 15. Allan GG, Peyron M (1995) Molecular weight manipulation of chitosan I: kinetics of depolymerization by nitrous acid. *Carbohydr. Res* 277: 257-272. [Link: https://goo.gl/SYFGle](https://goo.gl/SYFGle)
 16. Tanioka S, Matsui Y, Irie T, Tanigawa T, Tanaka Y, et al. (1996) Oxidative depolymerization of chitosan by hydroxyl radical. *Biosci Biotechnol Biochem* 60: 2001-2004. [Link: https://goo.gl/K7oAwN](https://goo.gl/K7oAwN)
 17. Chang KLB, Tai MC, Cheng FH (2001) Kinetics and products of the degradation of chitosan by hydrogen peroxide. *J Agric Food Chem* 49: 4845-4851. [Link: https://goo.gl/WTKmJR](https://goo.gl/WTKmJR)
 18. Croisier F, Jérôme C (2013) Chitosan-based biomaterials for tissue engineering. *Eur Polym J* 49: 780-792. [Link: https://goo.gl/qj4q0K](https://goo.gl/qj4q0K)
 19. Bodmeier R, Chen H, Paeratakul O (1989) A novel approach to the oral delivery of micro-or nanoparticles. *Pharm Res* 6: 413-417. [Link: https://goo.gl/L60C4n](https://goo.gl/L60C4n)
 20. Alonso MJ, Sánchez A (2003) The potential of chitosan in ocular drug delivery. *J. Pharm. Pharmacol.* 55: 1451-1463. [Link: https://goo.gl/Y9b6s1](https://goo.gl/Y9b6s1)
 21. Wu Y, Yang W, Wang C, Hu J, Fu S (2005) Chitosan nanoparticles as a novel delivery system for ammonium glycyrrhizinate. *Int J Pharm* 295: 235-245. [Link: https://goo.gl/M9jcgA](https://goo.gl/M9jcgA)
 22. Zhang H, Oh M, Allen C, Kumacheva E (2004) Monodisperse chitosan nanoparticles for mucosal drug delivery. *Biomacromolecules* 5: 2461-2468. [Link: https://goo.gl/6GSxeD](https://goo.gl/6GSxeD)
 23. Tsai ML, Bai SW, Chen RH (2008) Cavitation effects versus stretch effects resulted in different size and polydispersity of ionotropic gelation chitosan-sodium tripolyphosphate nanoparticle. *Carbohydr Polym* 71: 448-457. [Link: https://goo.gl/uqPUQg](https://goo.gl/uqPUQg)
 24. Wang W, Bo S, Li S, Qin W (1991) Determination of the Mark-Houwink equation for chitosans with different degrees of deacetylation. *Int. J. Biol. Macromol.* 13: 281-285. [Link: https://goo.gl/S2Qsvr](https://goo.gl/S2Qsvr)
 25. Roberts GAF, Domszy JG (1982) Determination of the viscometric constants for chitosan. *Int J Biol Macromol* 4: 374-377. [Link: https://goo.gl/uwYuPq](https://goo.gl/uwYuPq)
 26. Sureshkumar MK, Das D, Mallia MB, Gupta P (2010) Adsorption of uranium from aqueous solution using chitosan-tripolyphosphate (CTPP) beads. *J Hazard Mater* 184: 65-72. [Link: https://goo.gl/9MHQTX](https://goo.gl/9MHQTX)
 27. Tang ESK, Huang M, Lim LY (2003) Ultrasonication of chitosan and chitosan nanoparticles. *Int J Pharm* 265: 103-114. [Link: https://goo.gl/MDzNRo](https://goo.gl/MDzNRo)
 28. Kara F, Aksoy EA, Yuksekdog Z, Hasirci N, Aksoy S (2014) Synthesis and surface modification of polyurethanes with chitosan for antibacterial properties. *Carbohydr Polym* 112: 39-47. [Link: https://goo.gl/8GoXQQ](https://goo.gl/8GoXQQ)
 29. Taheri S, Sadeghi GMM (2015) Microstructure-property relationships of organomontmorillonite /polyurethane nanocomposites: Influence of hard segment content. *Appl Clay Sci* 114: 430-439. [Link: https://goo.gl/1ZRXu3](https://goo.gl/1ZRXu3)
 30. Ishiyama M, Tominaga H, Shiga M, Sasamoto K, Ohkura Y, et al. (1996) A combined assay of cell viability and in vitro cytotoxicity with a highly water-soluble tetrazolium salt, neutral red and crystal violet. *Biol Pharm Bull* 19: 1518-1520. [Link: https://goo.gl/5bZJzT](https://goo.gl/5bZJzT)
 31. Huang M, Khor E, Lim LY (2004) Uptake and cytotoxicity of chitosan molecules and nanoparticles: Effects of molecular weight and degree of deacetylation. *Pharm Res* 21: 344-353. [Link: https://goo.gl/iymKC9](https://goo.gl/iymKC9)
 32. Silva CM, Veiga F, Ribeiro AJ, Zerroukn N, Arnaud P (2006) Effect of chitosan-coated alginate microspheres on the permeability of Caco-2 cell monolayers. *Drug Dev Ind Pharm* 32: 1079-1088. [Link: https://goo.gl/Bpa2iL](https://goo.gl/Bpa2iL)